

# Quantum dynamics of exchange biased Single Molecule Magnets

W. Wernsdorfer<sup>a</sup> N. Aliaga-Alcalde<sup>b</sup> R. Tiron<sup>a</sup> D. N. Hendrickson<sup>c</sup> G. Christou<sup>b</sup>

<sup>a</sup>Lab. Louis Néel, CNRS, BP 166, 38042 Grenoble Cedex 9, France

<sup>b</sup>Dept. of Chemistry, University of Florida, Gainesville, Florida 32611-7200

<sup>c</sup>Dept. of Chemistry and Biochemistry, University of California at San Diego, La Jolla, California 92093-0358

---

## Abstract

We present a new family of exchange biased Single Molecule Magnets in which antiferromagnetic coupling between the two components results in quantum behaviour different from that of the individual SMMs. Our experimental observations and theoretical analysis suggest a means of tuning the quantum tunnelling of magnetization in SMMs.

*Key words:* Single Molecule Magnets, quantum tunneling, exchange bias, dimer

*PACS:* 75.45.+j, 75.60.Ej

---

Various present and future specialized applications of magnets require monodisperse, small magnetic particles, and the discovery of molecules that can function as nanoscale magnets was an important development in this regard [1]. These molecules act as single-domain magnetic particles that, below their blocking temperature, exhibit magnetization hysteresis, a classical property of macroscopic magnets. Such single-molecule magnets (SMMs) [2] straddle the interface between classical and quantum mechanical behaviour because they also display quantum tunnelling of magnetization [3,4,5,6,7,8,9] and quantum phase interference [10,11]. Quantum tunnelling of magnetization can be advantageous for some potential applications of SMMs, for example, in providing the quantum superposition of states required for quantum computing. However, it is a disadvantage in other applications, such as information storage, where it would lead to information loss. Thus it is important to both understand and control the

quantum properties of SMMs. Here we present a new family of supramolecular SMM dimers [12] in which antiferromagnetic coupling between the two components results in quantum behaviour different from that of the individual SMMs. Our experimental observations and theoretical analysis suggest a means of tuning the quantum tunnelling of magnetization in SMMs.

The compound has the formula

$[\text{Mn}_4\text{O}_3\text{Cl}_4(\text{O}_2\text{CEt})_3(\text{py})_3]$  (hereafter  $\text{Mn}_4$ ). The preparation, X-ray structure, and detailed physical characterization have been reported [13,14]. The complex has a distorted cubane-like core geometry and is  $\text{Mn}_3^{\text{III}}\text{Mn}^{\text{IV}}$ . Strong superexchange coupling between the spins leads to a well isolated  $S = 9/2$  ground state.  $\text{Mn}_4$  crystallizes in the hexagonal space group  $R\bar{3}(\text{m})$  with pairs of  $\text{Mn}_4$  molecules lying head-to-head on a crystallographic  $S_6$  symmetry axis (Fig. 1). Thus, each  $\text{M}_4$  has  $C_3$  symmetry and the  $[\text{Mn}_4]_2$  dimer has  $S_6$  symmetry. This supramolecular ar-

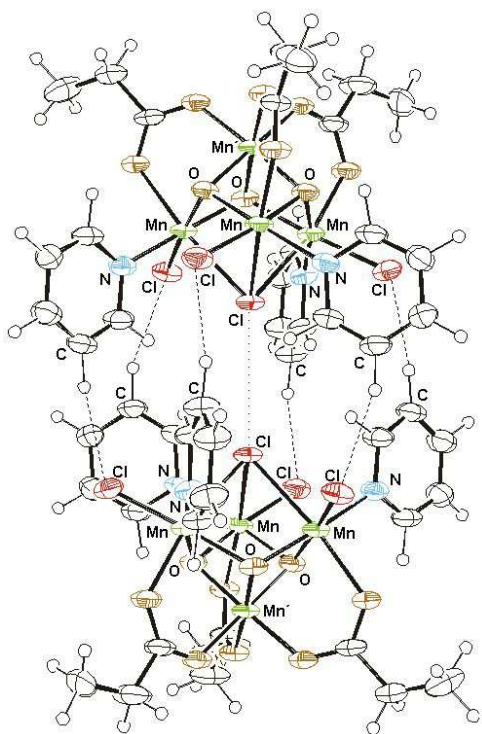


Fig. 1. The structure of the  $[\text{Mn}_4]_2$  dimer of  $[\text{Mn}_4\text{O}_3\text{Cl}_4(\text{O}_2\text{CEt})_3(\text{py})_3]$ . The small circles are hydrogen atoms. The dashed lines are C-H $\cdots$ Cl hydrogen bonds and the dotted line is the close Cl $\cdots$ Cl approach. The labels Mn and Mn' refer to Mn<sup>III</sup> and Mn<sup>IV</sup> ions, respectively.

arrangement is held together by six C-H $\cdots$ Cl hydrogen bonds (dashed lines in Fig. 1) between the pyridine (py) rings on one  $\text{Mn}_4$  and Cl ions on the other. The C-H $\cdots$ Cl hydrogen bonds in  $[\text{Mn}_4]_2$  have C $\cdots$ Cl distances and C-H $\cdots$ Cl angles of 0.371 nm and 161.57 $^\circ$ , respectively, typical of this type of hydrogen bond. The  $[\text{Mn}_4]_2$  dimer also brings the central bridging Cl ions of each  $\text{Mn}_4$  close together (0.3858 nm, dotted line in Fig. 1), almost at their Van der Waals separation (0.36 nm). Each  $[\text{Mn}_4]_2$  is rather well separated from neighboring dimers. The supramolecular linkage within  $[\text{Mn}_4]_2$  introduces exchange interactions between the  $\text{M}_4$  molecules via both the six C-H $\cdots$ Cl pathways and the Cl $\cdots$ Cl approach. All these seven interactions are expected to be weak, but combined they will lead to noticeable antiferromagnetic coupling between the  $\text{Mn}_4$  units.

Antiferromagnetic coupling between the  $\text{M}_4$

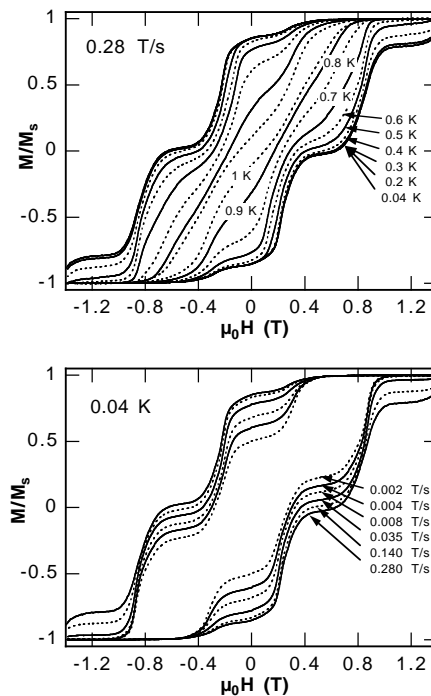


Fig. 2. Normalized magnetization versus applied magnetic field. The resulting hysteresis loops are shown at (a) different temperatures and (b) different field sweep rates. Note that the loops become temperature-independent below about 0.3 K but are still sweep-rate-dependent owing to resonant quantum tunnelling between discrete energy states of the  $[\text{Mn}_4]_2$  dimer.

units in  $[\text{Mn}_4]_2$  results in the latter being an excellent candidate for the study of quantum tunnelling in a system of truly identical, antiferromagnetically-coupled particles with a ground state  $S = 0$ . Such a system has long been sought for study after the theoretical conclusion [15] that tunnelling in antiferromagnets is much more pronounced than in ferromagnets.

Tunnelling studies on  $[\text{Mn}_4]_2$  were performed by magnetization measurements on single crystals using an array of micro-SQUIDs [16]. Fig. 2 shows typical hysteresis loops in magnetization versus magnetic field scans with the field applied nearly along the easy axis of magnetization of  $[\text{Mn}_4]_2$ , that is, parallel to the  $S_6$  axis [17]. These loops display step-like features separated by plateaus. The step heights are temperature-dependent above 0.3 K; below this, the loops become temperature-

independent. As discussed below, the steps are due to resonant quantum tunnelling of the magnetization (QTM) between the energy states of the  $[\text{Mn}_4]_2$  dimer.

QTM has been previously observed for several SMMs [3,4,5,6,7,8,9], but the novelty for  $[\text{Mn}_4]_2$  is that the QTM is now the collective behavior of the complete  $S = 0$  dimer of exchange-coupled  $S = 9/2$   $\text{Mn}_4$  quantum systems. This coupling is manifested as an exchange bias of all tunnelling transitions, and the resulting hysteresis loop consequently displays unique features, such as the absence for the first time in a SMM of a QTM step at zero field.

Before interpreting the hysteresis loops further, we discuss a simplified spin Hamiltonian describing the  $[\text{Mn}_4]_2$  dimer. Each  $\text{M}_4$  SMM can be modeled as a giant spin of  $S = 9/2$  with Ising-like anisotropy. The corresponding Hamiltonian is given by

$$\mathcal{H}_i = -DS_{z,i}^2 + \mathcal{H}_{\text{trans},i} + g\mu_B\mu_0\mathbf{S}_i \cdot \mathbf{H} \quad (1)$$

where  $i = 1$  or  $2$  (referring to the two  $\text{M}_4$  SMMs of the dimer),  $D$  is the uniaxial anisotropy constant, and the other symbols have their usual meaning. Tunnelling is allowed in these half-integer ( $S = 9/2$ ) spin systems because of a small transverse anisotropy  $\mathcal{H}_{\text{trans},i}$  contains  $S_{x,i}$  and  $S_{y,i}$  spin operators and transverse fields ( $H_x$  and  $H_y$ ). The exact form of  $\mathcal{H}_{\text{trans},i}$  is not important in this discussion. The last term in Eq. 1 is the Zeeman energy associated with an applied field. The  $\text{Mn}_4$  units within the  $[\text{Mn}_4]_2$  dimer are coupled by a weak superexchange interaction  $J$  via both the six C-H $\cdots$ Cl pathways and the Cl $\cdots$ Cl approach. Thus, the Hamiltonian ( $\mathcal{H}$ ) for  $[\text{Mn}_4]_2$  is

$$\mathcal{H} = \mathcal{H}_1 + \mathcal{H}_2 + JS_1 \cdot S_2 \quad (2)$$

where  $S_1 = S_2 = 9/2$ . The  $(2S_1 + 1)(2S_2 + 1) = 100$  energy states of the dimer can be calculated by exact diagonalization and are plotted in Fig. 3a as a function of applied field along the easy axis. Each state of  $[\text{Mn}_4]_2$  can be labelled by two quantum numbers ( $M_1, M_2$ ) for the two  $\text{Mn}_4$  SMMs, with  $M_1 = -9/2, -7/2, \dots, 9/2$  and  $M_2 = -9/2, -7/2, \dots, 9/2$ . For the sake of simplicity, we do not discuss the mixing with other spin states

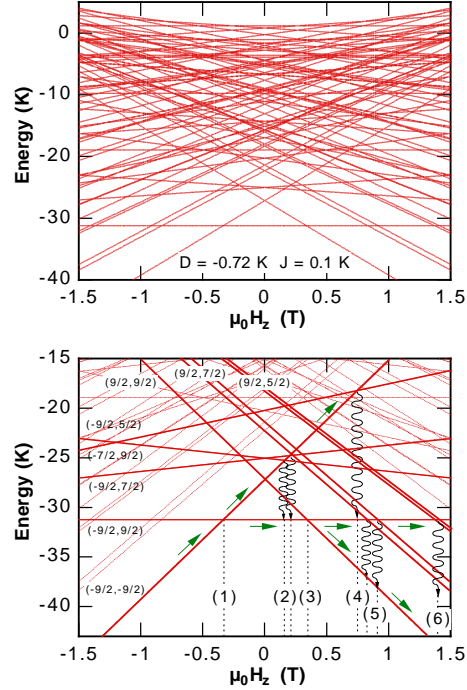


Fig. 3. The spin state energies of  $[\text{Mn}_4]_2$  as a function of applied magnetic field. (a) Energy vs field plot for the 100 states of the exchange-coupled dimer of two spin  $S = 9/2$   $\text{Mn}_4$  units. Transverse terms in  $\mathcal{H}_{\text{trans},i}$  are neglected for the sake of simplicity. However, transverse exchange coupling terms are included. (b) Enlargement of Fig. 3a showing only levels populated at very low temperature. Dotted lines, labelled (1) to (6), indicate the strongest tunnel resonances: (1)  $(-9/2, -9/2)$  to  $(-9/2, 9/2)$ ; (2)  $(-9/2, -9/2)$  to  $(-9/2, 7/2)$ , followed by relaxation to  $(-9/2, 9/2)$ ; (3)  $(-9/2, 9/2)$  to  $(9/2, 9/2)$ ; (4)  $(-9/2, -9/2)$  to  $(-9/2, 5/2)$ , followed by relaxation to  $(-9/2, 9/2)$ ; (5)  $(-9/2, 9/2)$  to  $(7/2, 9/2)$ , followed by relaxation to  $(9/2, 9/2)$ . (6)  $(-9/2, 9/2)$  to  $(5/2, 9/2)$ , followed by relaxation to  $(9/2, 9/2)$ . For clarity, degenerate states such as  $(M, M')$  and  $(M', M)$  are not both listed.

that is due to transverse anisotropy terms, that is  $\mathcal{H}_{\text{trans},i} = 0$ .

At very low temperature, most of the excited spin states are not populated and can be neglected. Thus, Fig. 3b shows only the low-lying states involved in the magnetization reversal at very low temperature when sweeping the field from a high negative field to a positive one. At high negative field, the initial state is  $(M_1, M_2) = (-9/2, -9/2)$ , that is, both molecules are in the negative ground

state. As the field is swept, the first (avoided) level crossing is at -0.33 Tesla. There is a non-zero probability, which depends upon the sweep rate, for the magnetization to tunnel from  $(-9/2, -9/2)$  to  $(-9/2, 9/2)$ . (For convenience, we do not list here (or below) both degenerate  $(M, M')$  and  $(M', M)$  states). The smaller the sweep rate the larger is the tunnelling probability, i.e. the larger is the resulting step in Fig. 2b. At field values away from the avoided level crossing, the dimer states are frozen by the significant magnetic anisotropy barrier.

At the next level crossing at 0 T, there is the possibility of tunnelling from  $(-9/2, -9/2)$  to  $(9/2, 9/2)$ , but this requires both  $\text{Mn}_4$  molecules of the dimer to tunnel simultaneously. The corresponding tunnelling probability is very small and can hardly be seen in Fig. 2. At the next level crossing at 0.2 T, the dimer can undergo tunnelling from  $(-9/2, -9/2)$  to  $(-9/2, 7/2)$ , corresponding to one of the  $\text{Mn}_4$  molecules tunnelling from the ground state to an excited state, followed by rapid relaxation from  $(-9/2, 7/2)$  to  $(-9/2, 9/2)$  (curly arrow in Fig. 3b). At the next level crossing at 0.33 T, the situation is analogous to that at -0.33 T, and the dimer can undergo tunnelling from  $(-9/2, 9/2)$  to  $(9/2, 9/2)$ . Between 0.33 and 0.75 T, there are several level crossings from  $(-9/2, -9/2)$  to excited states that require simultaneous tunnelling in both  $\text{Mn}_4$  units and can be neglected. The level crossing at 0.75 T allows tunnelling from  $(-9/2, -9/2)$  to  $(-9/2, 5/2)$ , followed by relaxation from  $(-9/2, 5/2)$  to  $(-9/2, 7/2)$  and  $(-9/2, 9/2)$ . At 0.87 T tunnelling can occur from  $(-9/2, 9/2)$  to  $(7/2, 9/2)$ , followed by relaxation from  $(7/2, 9/2)$  to  $(9/2, 9/2)$ . Finally, at 1.4 T tunnelling can occur from  $(-9/2, 9/2)$  to  $(5/2, 9/2)$ , followed by relaxation from  $(5/2, 9/2)$  to  $(9/2, 9/2)$ . The values of  $D$  and  $J$  used in Fig. 3 were calculated from the field positions of the steps in the hysteresis loops, ignoring transverse (and fourth order) anisotropy terms. The calculated values are  $D \approx -0.72$  K and  $J \approx +0.1$  K. The former is very close to those determined experimentally for several (isolated)  $\text{Mn}_4$  SMMs [18,19], and the latter is antiferromagnetic (positive value) and very weak, as expected for an exchange interaction via the six C-H  $\cdot\cdot$  Cl and the Cl  $\cdot\cdot$  Cl pathways. A value of  $J \approx 0.1$  K was also obtained

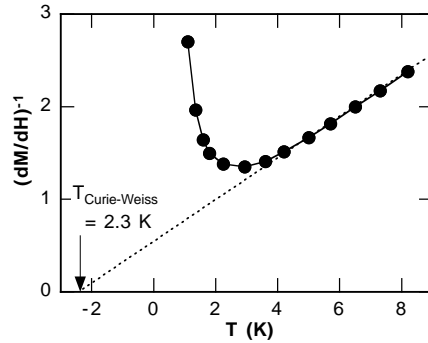


Fig. 4. Inverse zero field susceptibility,  $dM/dH^{-1}$  ( $H = 0$ ), versus temperature, determined using hysteresis loops. The negative Curie-Weiss constant of 2.3 K is in good agreement with an antiferromagnetic coupling of  $J \approx 0.1$  K.

from susceptibility determinations using hysteresis loops measured in the 1 to 8 K range (Fig. 4).

We tried to get a deeper insight into the relaxation processes by relaxation measurements at constant applied field for initially saturated or demagnetized magnetization (Fig. 5). The relaxation paths of the former are analogous to those of hysteresis loops (Fig. 2) whereas the latter starts in an initial state of  $(-9/2, 9/2)$  for nearly all dimers. Thus, transitions (2) and (4) should not occur that can be seen well in Fig. 5. Furthermore, this shows that only few dimers relax via transitions (4) of initially saturated magnetization. Note that all transitions are not well resolved, due to significant broadening by dipolar effects and small exchange coupling between neighboring dimers.

Relaxation data were determined from DC relaxation decay measurements: first a field of 1.4 T was applied to the sample at 5 K to saturate the magnetization in one direction, and the temperature lowered to a chosen value between 1 and 0.04 K. The field was then swept to 0 T at 0.28 T/s and the magnetization in zero field measured as a function of time (Fig. 6). From these data, relaxation times could be extracted which allows the construction of an Arrhenius plot (Fig. 7) which contains several distinct features. Above ca. 0.3 K the relaxation rate is temperature-dependent with  $\tau_0 = 3.8 \times 10^{-6}$  s and  $U_{\text{eff}} = 10.7$  K. Below ca. 0.3 K however, the relaxation rate is temperature-independent with a relaxation rate of  $8 \times 10^5$  s in-

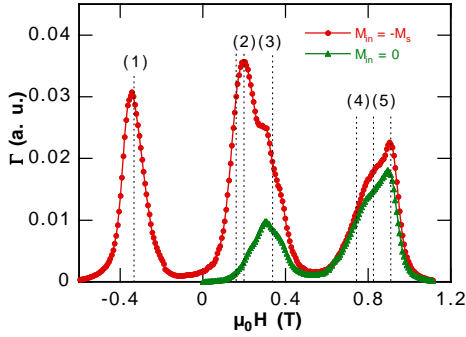


Fig. 5. Relaxation rate versus applied field for initially saturated or demagnetized magnetization. The dominating tunnel transitions are indicated by dashed lines and numbers (1) to (5), which are indicated in Fig.3b and explained in the text. The dashed lines are at positions calculated from Fig. 3b.

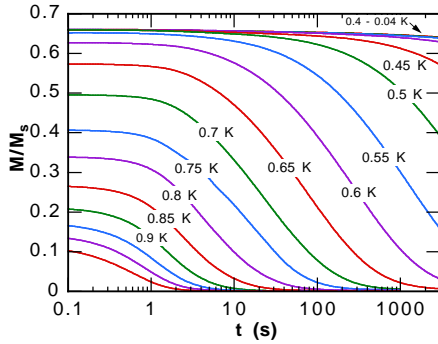


Fig. 6. Relaxation measurements at zero applied field at several temperatures.

dicative of QTM between the ground states.

The above results demonstrate that even weak exchange interactions can have a large influence on the quantum properties of SMMs. From one viewpoint, each half of the  $[\text{Mn}_4]_2$  dimer acts as a field bias on its neighbor, shifting the tunnel resonances to new positions relative to isolated  $\text{Mn}_4$  molecules. In particular, the latter show a strong QTM step at zero field in the hysteresis loop [18], a feature absent for  $[\text{Mn}_4]_2$  (Fig. 2) because this would be a double quantum transition with a very low probability of occurrence. The absence of tunnelling at zero-field is important if SMMs are to be used for information storage, and the option is still retained to switch on tunnelling, if and when required, by application of a field. Thus, future stud-

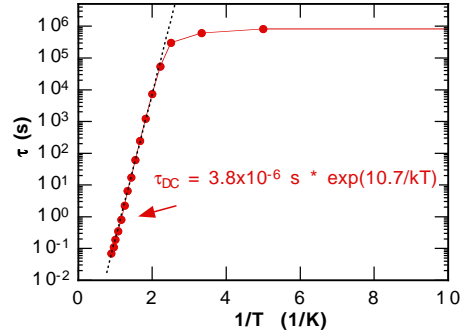


Fig. 7. Arrhenius plot of the relaxations times  $\tau$  versus the inverse temperature.

ies will probe this double transition at zero field in  $[\text{Mn}_4]_2$ , and the corresponding multiple quantum transition in higher supramolecular aggregates of SMMs, including determining their exact probability of occurrence and to what extent this can be controlled by the degree of aggregation, variation of exchange coupling strength, and similar modifications. From another viewpoint,  $[\text{Mn}_4]_2$  represents an unequivocal and unprecedented example of quantum tunnelling in a monodisperse antiferromagnet with no uncompensated spin (i.e.  $S = 0$ ) in the ground state. Thus,  $[\text{Mn}_4]_2$  and related species will prove invaluable for detailed studies of this phenomenon. Finally, the absence of a level crossing at zero field also makes the  $[\text{Mn}_4]_2$  dimer a very interesting candidate as a qubit for quantum computing, because the ground state is the entangled combination of the  $(9/2, -9/2)$  and  $(-9/2, 9/2)$  states; the coupling of this  $S = 0$  system to environmental degrees of freedom should be small, which means decoherence effects should also be small.

In future work, we shall use the Landau-Zener method to determine the tunnel splitting in  $[\text{Mn}_4]_2$ , and apply a transverse field to probe its exact influence on QTM rates (we have already confirmed that a transverse field increases the tunnelling rate, as expected for QTM). The identification of both an antiferromagnetic coupling and an exchange-bias effect in  $[\text{Mn}_4]_2$  demonstrates the feasibility of employing supramolecular chemistry for modulating the quantum physics of SMMs, providing a realistic general method to fine-tune

the properties of these molecular nanoscale materials. This brings closer their use in devices.

## References

- [1] R. Sessoli, *et al.*, J. Am. Chem. Soc. 115 (1993) 1804–1816.
- [2] S. M. J. Aubin, *et al.*, Distorted cubane complexes as single-molecule magnets, J. Am. Chem. Soc. 118 (1996) 7746.
- [3] M. Novak, R. Sessoli, in: L. Gunther, B. Barbara (Eds.), Quantum Tunneling of Magnetization-QTM'94, Vol. 301 of NATO ASI Series E: Applied Sciences, Kluwer Academic Publishers, London, 1995, pp. 171–188.
- [4] J. R. Friedman, *et al.*, Phys. Rev. Lett. 76 (1996) 3830.
- [5] L. Thomas, *et al.*, Nature (London) 383 (1996) 145.
- [6] C. Sangregorio, *et al.*, Phys. Rev. Lett. 78 (1997) 4645.
- [7] S. M. J. Aubin, *et al.*, J. Am. Chem. Soc. 120 (1998) 839.
- [8] D. J. Price, *et al.*, Phil. Trans. R. Soc. Lond. A 357 (1999) 3099.
- [9] J. Yoo, *et al.*, Inorg. Chem. 39 (2000) 3615.
- [10] W. Wernsdorfer, R. Sessoli, Science 284 (1999) 133.
- [11] A. Garg, EuroPhys. Lett. 22 (1993) 205.
- [12] W. Wernsdorfer, N. Aliaga-Alcalde, D. Hendrickson, G. Christou, Nature 416 (2002) 406.
- [13] D. N. Hendrickson, *et al.*, J. Am. Chem. Soc. 114 (1992) 2455.
- [14] N. Aliaga-Alcalde, *et al.*, to be published.
- [15] B. Barbara, E. Chudnovsky, Phys. Lett. A 145 (1990) 205.
- [16] W. Wernsdorfer, Adv. Chem. Phys. 118 (2001) 99.
- [17] The main difference between the hysteresis loops presented here and in the original paper [12] concerns a better alignment of the applied field.
- [18] S. M. J. Aubin, *et al.*, J. Am. Chem. Soc. 120 (1998) 4991.
- [19] H. Andres, *et al.*, J. Am. Chem. Soc. 122 (2000) 12469.